Computers and Geotechnics, Vol. 22, No. 2, pp. 135–151, 1998

Printed in Great Britain
PII: S0266-352X(98)00003-2
0266-352X/98/$19.00 + 0.00

A Continuum Damage Constitutive Law for Brittle Rocks

F. Homand-Etienne,[a]* D. Hoxha[a] & J. F. Shao[b]

[a]LAEGO, ENSGéologie, Vandoeuvre-lès-Nancy, France
[b]LML-URA 1441, CNRS, University of Lille I, Eudil, Villeneuve d'Ascq, France

(Received 24 January 1997; revised version received 4 January 1998; accepted 16 January 1998)

ABSTRACT

The non-linear mechanical behaviour of two different granites was investigated. Short term triaxial tests have been performed in order to study the short term behaviour (instantaneous growth of cracks) of the rock. A continuous damage model is then proposed. The internal damage variable is directly related to the second order crack density tensor used by Kachanov in the study of effective elastic properties of cracked solids. An instantaneous crack growth criterion has been used to describe the time-independent evolution of the damage tensor. The verification of the model has been performed for various loading paths. The results of a numerical modelling show that it is possible to reproduce most of the observable characteristics of damaged zone around an underground opening excavated into brittle rocks.

INTRODUCTION

Under high *in situ* stresses and highly anisotropic stress ratios, an excavation damaged zone (EDZ) may form around an underground opening excavated into brittle rocks, even by using an excavation method without explosives. The failure mechanism in this damaged zone is the initiation and growth of cracks and fractures and is directly related to the constitutive behaviour of rock mass. Anisotropic damage modelling of brittle rocks is a recent research field and many theoretical and experimental investigations are in progress.

*To whom correspondence should be addressed.

Indeed, irreversible deformations and failure in brittle rocks subjected to compressive stresses, occur by progressive damage as microcracks initiate and grow on the small scale and coalesce to form large scale fractures and faults. Experimental studies on brittle rocks have shown that there are many different mechanisms by which cracks can be initiated and grown under compressive stresses [1–7]. These mechanisms include sliding along pre-existing cracks and grain boundaries, pore crushing, elastic mismatch between mineral grains and dislocation movement. The consequence of these process is a progressive degradation of the rock. Furthermore, the crack growth is of directional character which induces an anisotropy of rock behaviour. Another important feature of the rock deformation and failure in brittle rocks is the subcritical growth of cracks which induce the time-dependent character in rock behaviour. Different physical mechanisms of the subcritical growth have been discussed by Atkinson [8] and Atkinson and Meredith [9].

In order to describe non-linear rock deformation, micromechanical fracture models have been proposed. A quite complete review was given by Kemeny and Cook [10]. In these models, crack growth conditions are obtained from the principles of linear elastic fracture mechanics and the constitutive equations are evaluated using Castigliano's theorem. Therefore the evaluation of the effective elastic tensor is not systematic and the application to 3-D cases is difficult. Micromechanical damage models have been proposed by Ju and Lee [11–13]. The self-consistent method is employed for weakly interacting elliptical microcracks in anisotropic media. The microcrack-induced inelastic compliances are systematically derived in terms of anisotropic microcrack opening displacements. Microcrack kinetic equations are characterised through the use of fracture mechanics stability criteria. The main advantage of the micromechanical models is the ability to describe the microstructural microcrack kinetics. However it is often difficult to implement such models in a numerical code, especially for 3D problems. On the other hand, anisotropic continuous damage models have also been developed (e.g. [11, 14–17]). These models are based on the thermodynamic principles and use an internal variable to describe the damage state of the rock. The numerical implementation of such models is usually easy. Moreover, although these models are identified from the macroscopic behaviour of the rock, it is possible to relate the internal damage variable to the microstructural mechanism of crack growth in order to make the models physically well funded.

In this paper, the non-linear deformation of two different granites is investigated. Short term triaxial tests have been performed in order to study the short term behaviour (instantaneous growth of cracks) of the rock. A continuous damage model will then be proposed. The internal damage variable is directly related to the second order crack density tensor used by Kachanov [18] in the study of effective elastic properties of cracked solids. An instantaneous crack growth criterion is used to describe the time-independent evolution of the damage tensor. Verification of the model is presented for various loading paths. Results of a numerical modelling show that it is possible to reproduce most of the observable characteristics of damaged zone (EDZ) around an underground opening excavated into brittle rocks.

EXPERIMENTAL STUDY

The studied rocks are the Lac du Bonnet granite and the Aspö diorite. The Lac du Bonnet granite is mainly composed of quartz, K-feldspar, plagioclase and biotite. The Aspö diorite is mainly composed of plagioclase and biotite and contains less quartz and K-feldspar and amphibole. Their mineralogy is approximately the same but the first rock contains more quartz than the second one. Grain size of the Lac du Bonnet granite is relatively homogeneous and ranged from 0.1 mm up to 3–4 mm. K-feldspar grain size of the Aspö diorite occurs as large as 6–7 mm crystals, but they are never joined; the other minerals are smaller (< 0.1 mm up to 1.5–2 mm).

Triaxial compression tests have first been performed with confining pressures of 0, 2, 5, 10, 20 and 40 MPa. In Figs 1 and 2, typical stress–strain curves are shown for the two rocks. Unloading–reloading cycles were included in order to determine the variation of the elastic modulus of the damaged rock. Generally there is a strong hysteresis phenomenon during unloading and reloading. In order to reduce the hysteresis loop and to make easier the determination of the effective modulus, a relaxation period is used before each unloading.

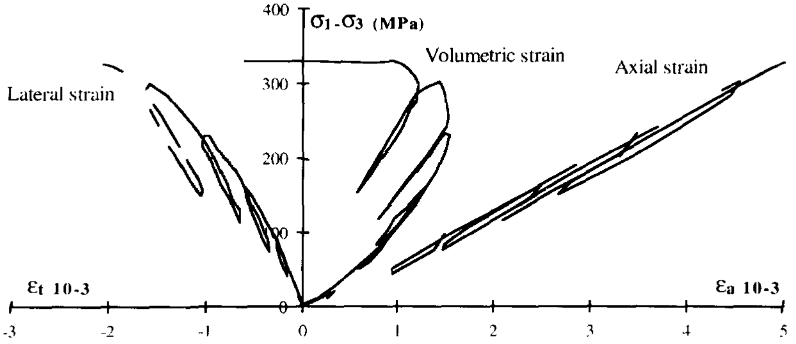

Fig. 1. Typical stress–strain curves of Lac du Bonnet granite in triaxial compression tests with unloading–reloading cycles ($\sigma_c = 20$ MPa).

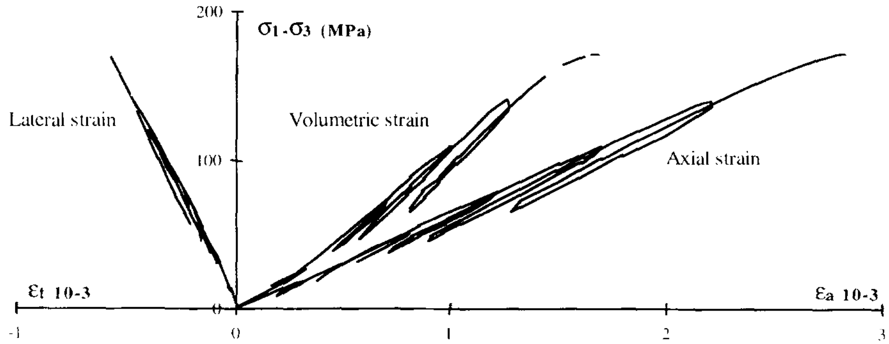

Fig. 2. Typical stress–strain curves of Aspö diorite in triaxial compression tests with unloading–reloading cycles ($\sigma_c = 5\,\mathrm{MPa}$).

From the stress-strain curves some remarks can be formulated. (1) The lateral strain ($\varepsilon 3$) presents a stronger non linearity than the axial strain ($\varepsilon 1$), and therefore the volumetric dilatancy is generally obtained. This is due to the crack growth in the axial direction. (2) By analysing the obtained results, it is noted that the effective modulus decreases as the damage grows. The damaged behaviour is transversely isotropic. (3) Although the use of relaxation period, hysteresis loops look still important. This may be explained by the time-dependent crack growth and internal friction effects in the rock during the unloading. Moreover, it seems that the hysteresis loop is more important when the confining pressure is smaller.

Furthermore other mechanical tests have been performed: three points bend, lateral extension and proportional triaxial tests. The results will be comment respectively in the identification of the model parameters part and in the validation of the model part.

ANISOTROPIC CONTINUOUS DAMAGE MODEL

Damage tensor

One of the key points in the formulation of an anisotropic damage model is to choose a suitable damage variable. Based on the work of Hill [19], by analysing the complementary energy density of a cracked solid, Kachanov [18] has shown that the elastic potential modification due to cracks can be expressed as function of some crack density tensor. In the case of opening and non-interacting cracks, the use of a second order tensor gives a rigorous characterisation of a crack array in the 2-D case and a good approximation in the 3-D case. The present study being limited to penny-shaped cracks, the following second order damage tensor is proposed:

$$\overline{\overline{D}} = \sum_j \hat{d}_j(s)(\bar{n} \otimes \bar{n})_j \tag{1}$$

with

$$\hat{d}_j(s) = \left[\frac{\hat{a}^3 - a_0^3}{a_0^3}\right]_j \text{ for the 3-D case}$$

and

$$\hat{d}_j(s) = \left[\frac{\hat{a}^2 - a_0^2}{a_0^2}\right]_j \text{ for the 2-D case}$$

In these equations, a_0 is the initial radius of cracks which is supposed uniform in undamaged rocks. $\hat{a}$ is the statistical average radius of the *jth* set of cracks. $\hat{d}_j(s)$ is considered as the relative evolution of crack density induced by applied stresses and subcritical microcrack growth. The use of such a relative density allows to bring a macroscopic character to the damage tensor $\overline{\overline{D}}$. Indeed, the representative volume element (RVE) concept is not directly implied in $\overline{\overline{D}}$ which is an internal state variable to define the material damage. In addition, only the sets of opening microcracks ($K_I > 0$) are accounted for in evaluating the damage tensor $\overline{\overline{D}}$.

Crack growth criteria and damage evolution

Two kinds of crack growth criteria, mechanical growth due to stress variations and subcritical growth due to stress corrosion, are taken into consideration in fracture mechanics. The first type of growth is only considered in this paper. By supposing that the crack growth occurs in tensile mode (mode I), the stress intensity factor K_I for a crack distribution, with $\hat{a}$ being the statistical average size of cracks with normal $\bar{n}$, may be approximated by:

$$K_I = \frac{2}{\pi}\sqrt{\pi\hat{a}}\left[\frac{\sigma_{kk}}{3} + f(\hat{a})\,\bar{n}\,\overline{\overline{S}}\,\bar{n}\right] \tag{2}$$

where $\overline{\overline{S}}$ is the deviatoric stress tensor $S_{ij} = \sigma_{ij} - (\sigma_{kk}/3)\delta_{ij}$. The presence of the mean stress term $\sigma_{kk}/3$ in the expression of K_I allows to account for the influence of the mean stress on the growth of microcracks. In fact, a positive (tensile) value of the mean stress increases K_I and thus favours crack growth. On the other hand, a negative (compression) value decreases K_I and thus prevents crack growth. Therefore, the mean stress is included in the expression of K_I in such a way that it will be possible to describe one of the basic characteristics of brittle rocks, the pressure sensitivity.

The choice of $f(\hat{a})$ function is essential and assumes two roles: First, $f(\hat{a})$ defines the proportionality between the applied deviatoric stress and the local tensile stress concentration due to the mechanisms of different nature (sliding of pre-existing cracks, pore crushing, elastic mismatch, etc.). Second, the $f(\hat{a})$ assumes the passage of stable crack growth to an unstable one. In the domain of stable crack growth, the local induced tensile stress, becomes smaller as the cracks grown on. So, $f(\hat{a})$ must be a decreased function of $\hat{a}$ in this domain. Otherwise, beyond some critical cracks length the unstable crack growth takes place, and $f(\hat{a})$ has to increase with the crack growth.

Since $f(\hat{a})$ stands for all the mechanisms of local stress concentration, it is difficult to establish an expression of it in a physical ground. Some similar function has been proposed in similar conditions [15]. Nevertheless, some polynomial approximation of $f(\hat{a})$ would be useful. Note, that from the polynomes in $\hat{a}$, only a second degree polynome could fulfil the requirements of the $f(\hat{a})$ function. Consequently, the following function was chosen in this paper.

$$f_2(\hat{a}) = t\left[1 - \frac{(\hat{a} - b)^2}{a_0(a_0 - b)}\right] \tag{3}$$

where t is a constant of proportionality dimensionless, and b is a critical length.

The coalescence of microcracks may occur when $\hat{a}$ is close to b. The condition $\hat{a} = b$ is used as a criterion for unstable failure of rock (onset of large scale fracture due to coalescence of microcracks) and is a natural upper limit of domain application of a continuous model, such as this one.

Mechanical growth of crack occurs when the stress factor intensity K_1 reaches a critical value K_{1C}:

$$K_1 = K_{1C} \tag{4}$$

For any stress state, the actual average size of the jth crack set, $\hat{a}_j$, in the direction $\bar{n}_j$ could be determinated from Eqns (2)–(4), and then the damage tensor $\overline{\overline{D}}$ could be calculated from (1).

Concerning the influence of confining pressure σ_C on $K_{1C}(\sigma_c = Abs(\sigma_1)$, with respect to our sign convention), experimental studies have shown that the crack growth rate is proportional to σ_C. Based on the experimental results [8, 20], the following equation is used:

$$K_{1C} = K_{1C}^0 + C\sigma_C \tag{5}$$

where C is a constant related to the rock and expressed in $\sqrt{m}$.

The K_{1C} increasing with respect to confining pressure σ_C is concomitant of changes of the material variables and state functions. Consequently, the energy release rate G should increase with respect to confining pressure. Moreover a parametric study [20] showed that parameter t is associated with an energy release rate. If K_{1C} increases with respect to σ_C (Eqn (5)), then t has to increase with respect to σ_C proportionally to C^2. The following relationship is suggested:

$$t = t_0 + C_1\sigma_C \tag{6}$$

where C_1 is the constant of proportionality expressed in MPa^{-1}.

In Fig. 3 the evolution of t with respect to σ_C is represented for Aspö diorite. The same results are obtained for the Lac du Bonnet granite, as well. This confirms the assumption Eqn (6) of the linearity of t with respect to σ_C, with the proportional coefficient approximately equal to C^2.

Thermodynamic potential and constitutive equations

In the case of non-interacting cracks, it has been shown [18,21], that the complementary strain energy should be a linear function of the damage tensor. Further, Dragon [17] proposed an original modification of Kachanov's work, by introducing a term relative to residual stress in the strain energy function which is expressed as follows:

$$w(\bar{\bar{\varepsilon}}, \bar{\bar{D}}) = gtr(\bar{\bar{\varepsilon}}.\bar{\bar{D}}) + \frac{1}{2}\lambda(tr\bar{\bar{\varepsilon}})^2 + \mu tr(\bar{\bar{\varepsilon}}.\bar{\bar{\varepsilon}}) + \alpha(tr\bar{\bar{\varepsilon}})tr(\bar{\bar{\varepsilon}}.\bar{\bar{D}}) + 2\beta tr(\bar{\bar{\varepsilon}}.\bar{\bar{\varepsilon}}.\bar{\bar{D}}) \tag{7}$$

where λ and μ are Lame's constants, g, α and β are three constants defining the damage induced modification of the strain energy. The term $gtr(\bar{\bar{\varepsilon}}.\bar{\bar{D}}$ in Eqn (7) allows to take into account the residual strain/stress effects without

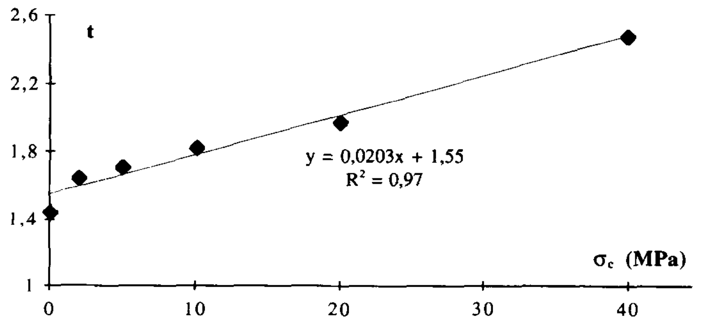

Fig. 3. Variation of t with respect to confining pressure for Aspö diorite.

explicit reference to plasticity concepts. By differentiating Eqn (7) with respect to $\bar{\bar{\varepsilon}}$ we obtain the constitutive equations as follows:

$$\bar{\bar{\sigma}} = \frac{\partial w}{\partial \varepsilon} = g\bar{\bar{D}} + \lambda(tr\bar{\bar{\varepsilon}})I + 2\mu\bar{\bar{\varepsilon}} + \alpha[tr(\bar{\bar{\varepsilon}}.\bar{\bar{D}})I + (tr\bar{\bar{\varepsilon}})\bar{\bar{D}}] + 2\beta(\bar{\bar{\varepsilon}}.\bar{\bar{D}} + \bar{\bar{D}}.\bar{\bar{\varepsilon}}) \quad (8)$$

By applying Eqn (8) to the case of conventional triaxial compression tests, the following stress strain relationships are obtained:

$$\begin{cases} \sigma_1 = gD_1 + (2\lambda + 2\mu + 4\alpha D_1 + 4\beta D_1)\varepsilon_1 + (\lambda + \alpha D_1)\varepsilon_3 \\ \sigma_3 = (2\lambda + 2\mu)\varepsilon_3 + (2\lambda + 2\alpha D_1)\varepsilon_1 \end{cases} \quad (9)$$

where $D_1 = D_2$ is the lateral component of the damage tensor and $D_3 = 0$. The assumption here is that the orientation of the dominant set of cracks (the vector normal of crack surface) is in the direction of the maximal principal stress.

Identification of the model parameters

The proposed damage model contains five parameters for the constitutive equation (λ,μ,g,α,β) and five others for the mechanical crack growth criterion (a_0, b, t_0, K^0_{IC}, C). All the parameters can be determined from standard laboratory tests.

The constant a_0 (initial crack size) is determined from a suitable microscopic analysis; a_0 is usually taken to be equal to the grain size. The parameter b may be considered as the critical crack length, i.e. the average crack length required for unstable failure of the rock through coalescence of microcracks. Consequently it is more suitable to calculate this parameter from the crack-coalescence stress (dilatancy) than to determine it from microscopic analysis. The parameter t_0 is easily calculated from beginning of dilation on lateral strain gauges, i.e. crack-initiation stress [20] using Eqn (2) with $\hat{a} = a_0$ as the crack growth has not yet begun.

K^0_{IC} is calculated from the experimental results of three point bend tests. Tests have shown that the crack growth rate is proportional to σ_C; the parameter C is calculated from the experimental results [Eqn (5)].

The parameters μ and λ are determined from the linear part of stress–strain curves in a triaxial test in a classical way since they are the elastic parameters. Note that the damage evolution is completely given by the criterion Eqn (2) and the damage tensor $\bar{\bar{D}}$ is known at each stress state through (1), as soon as the parameters involving in (2) are known. Then the values of g,α,β are obtained directly by solving a linear system of three equations, two resulting from (9), written for unloading slopes in the non-linear part of stress-deformation curves, and the other from the same unloading slopes written for an total unloading. The assumption here is that there is not instantaneous crack growth while in unloading. For the two tested rocks, the values of these parameters are presented in Table 1.

After the model parameters are determined, the verification of the model is made for triaxial compression tests with various confining pressures. The comparisons between the data and model prediction show a general good agreement (Fig. 4).

VALIDATION OF THE MODEL

It is more of interest to check the performance of the model on proportional triaxial and lateral extension tests because these paths are different from those used to identify the model parameters. As it is shown in Fig. 5, where are plotted the stress–axial and lateral strains curves for a proportional triaxial test ($\sigma_1/\sigma_3 = 10$), model prediction concerning the strength are satisfying. Concerning the lateral strains, the prediction are not quite consistent with the experimental results.

In Figs 6 and 7, reduced lateral extension tests (confining pressure is reduced while axial stress is kept constant) are simulated by means of the model. A good agreement between the numerical predictions and experimental data is obtained, except for the transversal strains. The beginning of the experimental stress–axial strain curves presents a phenomenon attributed to time-dependent deformations. When subtracting these deformations, the predicted curve fits perfectly to the experimental curve (Fig. 8).

STABILITY OF A ROCK MASS EVALUATED BY UDEC WITH OUR DAMAGE MODEL

Implementation in UDEC

The Discrete Element Method is frequently used in rock mechanics because of a powerful discontinum modelling approach for simulating the behaviour

TABLE 1
Parameters of the damage model

	a_0 (mm)	t_0	b/a_0	K_{IC}^0 ($MPa\sqrt{m}$)	C ($\sqrt{m}$)	α (MPa)	β (MPa)	g (MPa)	E_0 (MPa)	ν_{00}
Lac du Bonnet	3	1.21	2.32	0.96	0.11	448	−1016	0	64000	0.28
Aspö	1.5	1.55	2.4	1.56	0.14	315	−955	−1.432	80000	0.21

of jointed rock masses. The calculations described in this paper were conducted using the two-dimensional UDEC code [22], first introduced by Cundall [23] and further developed by Cundall and others [24, 25]. This code was chosen because of possibilities to study the interaction of joints with the damage zone (subject of other studies) [26].

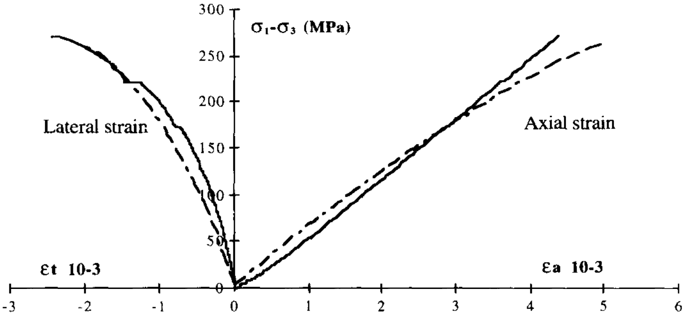

Fig. 4. Comparisons between the data (solid lines) and model prediction (broken lines) for a triaxial test ($\sigma_C = 10\,\text{MPa}$); Lac du Bonnet granite.

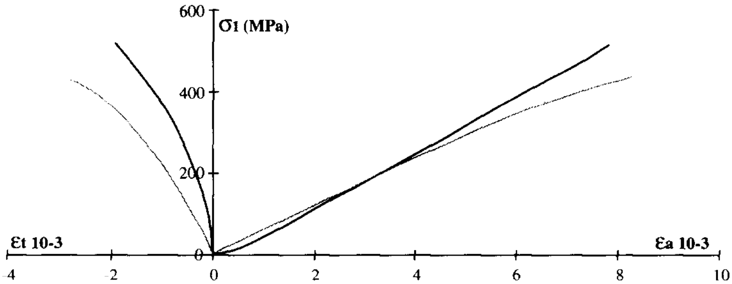

Fig. 5. Comparisons between the data (solid lines) and model prediction (broken lines) for a proportional triaxial test ($\sigma_3/\sigma_1 = 10$): Lac du Bonnet granite.

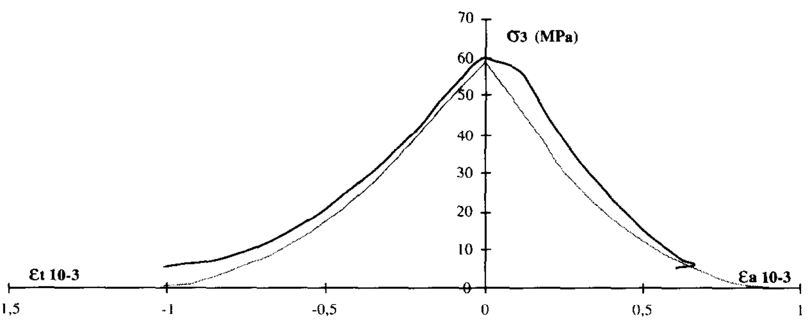

Fig. 6. Comparisons between the data (solid lines) and model prediction (broken lines) for a lateral reduced extension test: Lac du Bonnet granite.

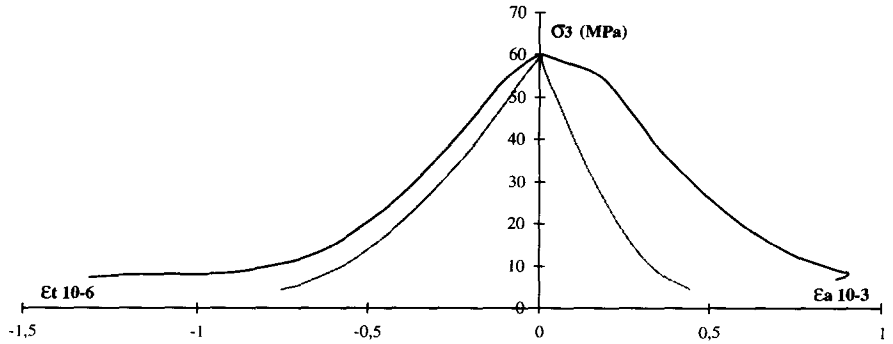

Fig. 7. Comparisons between the data (solid lines) and model prediction (broken lines) for a lateral reduced extension test: Aspö diorite.

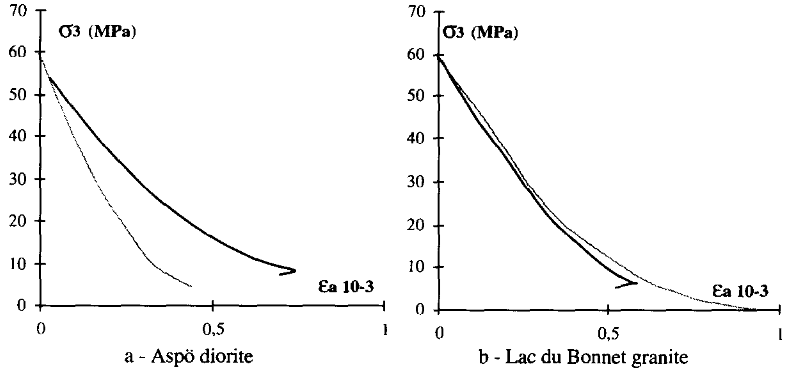

Fig. 8. Comparisons between the corriged data (solid lines) and model prediction (broken lines) for lateral reduced extension tests.

Here we assumed that the new strain increment ($\Delta\bar{\bar{\varepsilon}}$) are derived from nodal velocities, and we compute the current stress increment ($\Delta\bar{\bar{\sigma}}$) corresponding to the current time step (Δt) and stress tensor $\bar{\bar{\sigma}}$. The input parameters are current strain increment and material parameters. The output parameters are damage variables, stress increments, microcracks and coalescence indicators. Here is the pseudo-code implemented in UDEC:

For each element

1. Compute the stress increments using Eqn (8) based on the strain increments and actual $\bar{\bar{D}}$

For each crack set in the element

Compute K_{I} [Eqn (3) with old crack length]
Check if the growth of crack took place for the actual stress [Eqn (4)]
If YES: adjust the new average length of this family [Eqn (3)]
If NO: go to ***Next Element***;

If the coalescence takes place (condition $\hat{a}_j = b$), then cancel the element and go to ***Next Element***;

Next Crack Set;

Compute the new $\overline{\overline{D}}$ tensor damage for this element [Eqn (1)] and go to 1

Next Element;

Element "cancelling" is realised by applying a Null zone model in the sense of UDEC, which means applying a Null stress. This approach could have some difficulties to guarantee the numerical stability, but the reducing of mesh size helps in the stabilising process.

AECL's mine-by experiment

The mine-by experiment was conducted at the 420 level of the Underground Research Laboratory (URL-AECL, Pinnawa, Canada) to investigate the response induced in the rock mass by excavating a 3.5-m diameter circular tunnel using a non-explosive technique [27, 28].

The results from the experiment *in situ* show progressive failures in compressive regions around the tunnel (Fig. 9).

We have chosen this site to check the performance of our model for two principal reasons: first the specific condition of a highly anisotropic stress

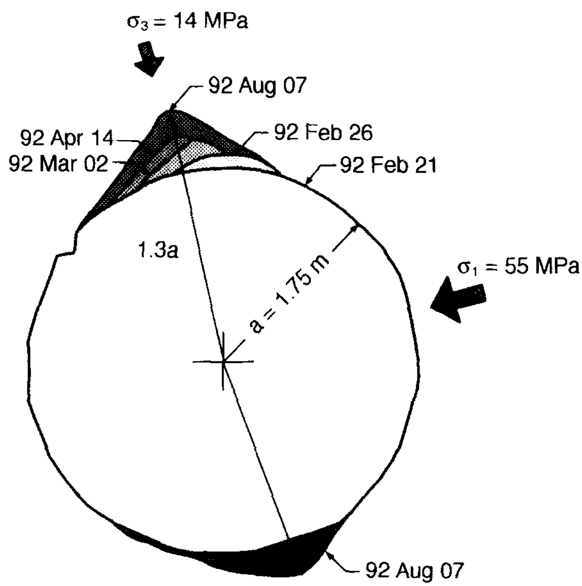

Fig. 9. Progressive development of breakout notch *in situ* in Lac du Bonnet granite (source Ref. [27]).

make this site a challenge for the numerical modelling, and second the site is very well documented [27, 28].

The stress tensor was considered as the following: $\sigma_1 = 55\,\text{MPa}$, $\sigma_2 = 48\,\text{MPa}$, and $\sigma_3 = 14\,\text{MPa}$, and the tunnel was designed to be approximately parallel to the intermediate principal stress direction. The input parameters are those catalogued in Table 1 for the Lac du Bonnet granite. Note, that the tested rock samples were not taken in the 420 m level, because of sampling difficulties, but in the 240 m level. So some minor differences in the characteristics of materials are expected.

Numerical results

The studied region was meshed regularly with rectangle elements. The size of elements increases progressively from the tunnel, trying to be as small as possible. In the case presented here there are in total some 96,000 elements. Before the excavation some 500 cycles are realised in order to establish the initial stability.

After the excavation, there are some zones in tension in the lateral part of the tunnel, however the first zones in coalescence appear in the zones of high compressive stress. The damaged zone grows on, and stability is reached after some 2000 cycles. The stability here means that the unbalanced force reaches some negligible values, and there are not the other zones passing the coalescence criterion in the last 200 cycles.

A simple representation of the tunnel profile at final stage is given in Figs 10 and 11 with the contours, respectively, of maximal active crack length and principal stress difference. The damaged regions have reached the coalescence, profiling a similar notch in the same places as in mine-by tunnel. The highly damaged zones are associated with the zones of highly compressive stress. The extent and the form of the simulated notch correspond quite well with the structures observed in the mine-by tunnel. The cracking process is developed all around the tunnel as well, but the length cracks do not fulfil yet the coalescence criterion (Fig. 10).

The depth of the notch reported to by Read and Martin [27], is ranged between 0.43 and 0.52 m and the calculation estimates the depth equal to 0.48 m.

The contours of principal stress difference are presented in Fig. 11. It could be noted that there is not a simple coincidence of the damaged zones with any contour of principal stress difference. However the maximal contour difference is just around the damaged zone.

In Fig. 12, radial displacements around the tunnel, for different angles in relation to the horizontal axis, are presented. The measures are realised by the extensometers placed all around the tunnel, before the excavation [27]. In the same graph we have superposed the prediction of our model. All the

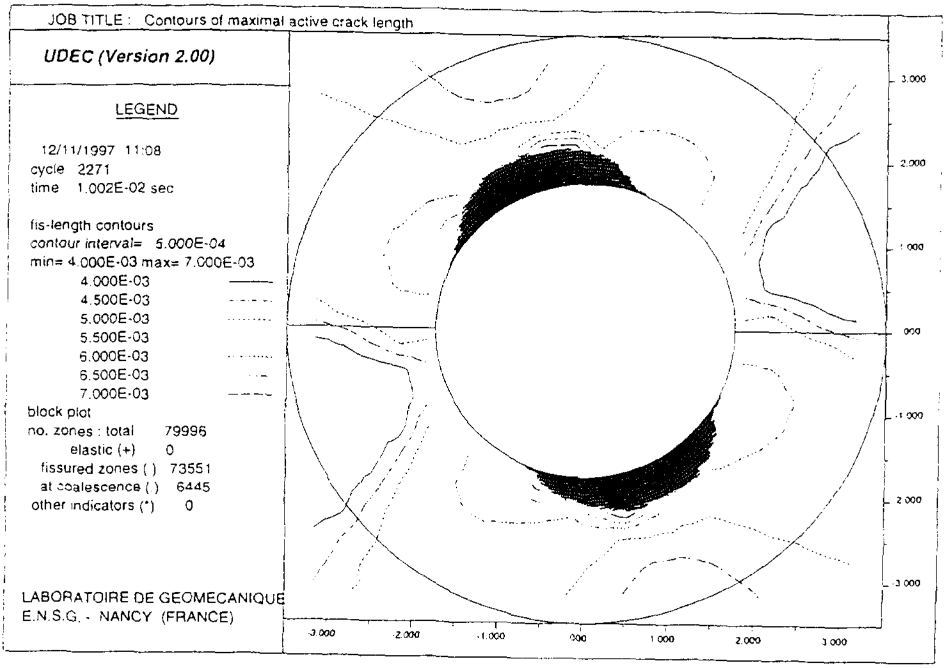

Fig. 10. Tunnel profile at final state and contours of maximal active crack length.

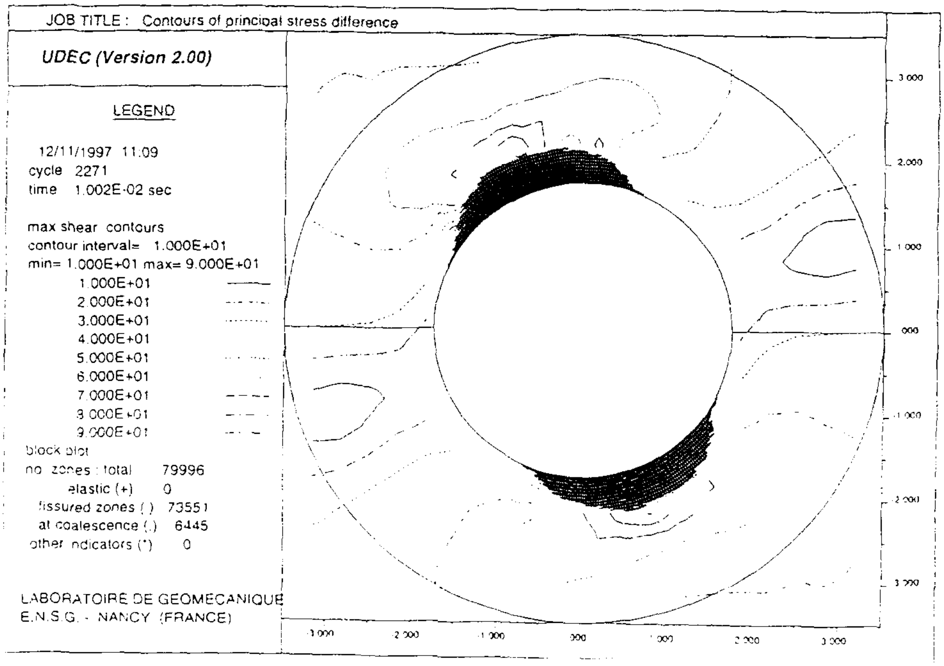

Fig. 11. Contours of principal stress difference.

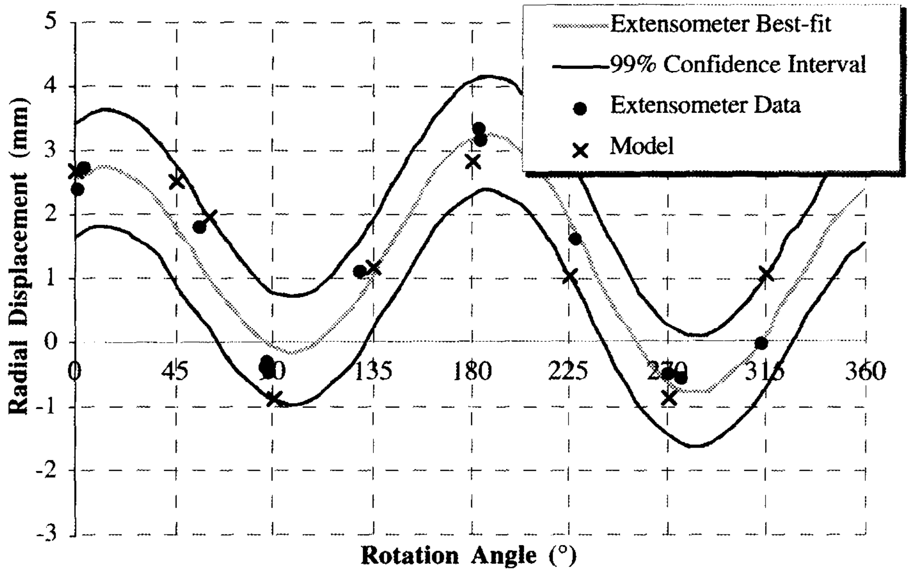

Fig. 12. Radial displacement from extensometers (source Ref. 27) and model prediction.

estimated values are in the 99% confidence interval drawn by Read and Martin and fit well the best-fit curve of measured data.

CONCLUSION

Triaxial compression tests have been used to show the non-linear deformation and damage in brittle rocks. The progressive microcrack growth in the axial direction results in a strong dilatancy and a transversely isotropic behaviour. A continuum damage mechanics approach is used to describe the time-independent mechanical growth due to stresses variation. The proposed continuous damage model is calibrated from short term triaxial tests. The verification of the model for various loading paths shows that a very good agreement between the experiments and model prediction have been obtained. The results of a numerical modelling show that it is possible to reproduce most of the observable characteristics of a damaged zone (EDZ) around an underground opening excavated into brittle rocks. All the parameters used are issued from mechanical tests and are entirely justified on physical grounds. However, it is possible to improve the model [29] by taking into account a second mechanism due to time-dependent subcritical growth due to stress corrosion.

ACKNOWLEDGEMENTS

The authors wish to acknowledge the Agence Nationale Pour la Gestion des Déchets Radioactifs (ANDRA) for financial support for this project.

REFERENCES

1. Wawersik, W. R. and Brace, W. F., Post-failure behavior of a granite and diabase. *Rock Mechanics*, 1971, **3**, 61–85.
2. Wong, T. F., Micromechanics of faulting in Westerly granite. *International Journal of Rock Mechanics and Mining Sciences*, 1982, **19**, 49–62.
3. Steif, P. S., Crack extension under compressive loading. *Engineering Fracture Mechanics*, 1984, **20**(3), 463–473.
4. Sammis, C. G. and Ashby, M. F., The failure of brittle porous solids under compressive stress states. *Acta metall.*, 1986, **34**(3), 511–526.
5. Fredrich, J. T. and Wong, T. F., Micromechanics of thermally induced cracking in three crustal rocks. *Journal of Geophysical Research*, 1986, **91**, 12743–12764.
6. Fredrich, J. T., Evans, B. and Wong, T. F., Micromechanics of the brittle to plastic transition in Carrara marble. *Journal of Geophysical Research*, 1989, **94**, 4129–4145.
7. Martin, C. D. and Chandler, N. A., The progressive failure of Lac du Bonnet granite. *International Journal of Rock Mechanics and Mining Sciences*, 1994, **31**, 643–659.
8. Atkinson, B. K., Subcritical crack growth in geological materials. *Journal of Geophysical Research*, 1984, **89**(B6), 4077–4114.
9. Atkinson, B. K. and Meredith, P. G., The theory of subcritical crack growth with applications to minerals and rocks. In *Fracture Mechanics of Rock*. ed. B. K. Atkinson. Academic Press, London, 1987, pp. 113–166.
10. Kemeny, J. M. and Cook, N. G. W., Micromechanics of deformation in rocks. In *Toughening Mechanics in Quasi-Brittle Materials*, ed. S. P. Shah. Kluwer Academic, 1991, pp. 155–188.
11. Ju, J. W., On the energy based coupled elastoplastic damage theories: constitutive modelling and computational aspects. *International Journal of Solids and Structures*, 1989, **25**(7), 803–833.
12. Ju, J. W. and Lee, X., Micromechanical damage model for brittle solids, I: tensile loadings. *Journal of Engineering Mechanics*, 1991, **117**(7), 1495–1514.
13. Lee, X. and Ju, J. W., Micromechanical damage model for brittle solids, I: tensile loadings. *Journal of Engineering Mechanics*, 1991, **117**(7), 1515–1536.
14. Krajcinovic, D. and Fonseka, G. U., The continuous damage theory of brittle materials. *Journal of Applied Mechanics*, 1981, **48**, 809–815.
15. Costin, L. S., Damage mechanics in the post failure regime. *Mechanics of Materials*, 1985, **4**, 149–160.
16. Singh, U. K. and Digby, P. J., A continuum damage model for simulation of the progressive failure of brittle rocks. *International Journal of Solids and Structures*, 1989, **25**(6), 647–663.
17. Dragon, A., Cormery, F., Désoyer, T. and Halm, D., Localized failure analysis using damage models. In *Localisation and Bifurcation Theory for Soils and*

Rocks, ed. R. Chambon, J. Desrues and I. Vardoulakis. Balkema, 1994, pp. 127–140.
18. Kachanov, M., Elastic solids with many cracks and related problems. *Advances in Apllied Mechanics*, 1994, **30**, 259–445.
19. Hill, R., Elastic properties of reinforced solids: some theoretical principles. *Journal of the Mechanics and Physics of Solids*, 1963, **11**, 357–372.
20. Hoxha, D. Endommagement des granites et stabilité des ouvrages souterrains: Thèse Doct. INPL, to be published.
21. Sayers, C. M. and Kachanov, M., A simple technique for finding effective elastic constants of cracked solids for arbitrary orientation statistics. *International Journal of Solids and Structures*, 1991, **27**(6), 671–680.
22. UDEC, *User's Manual*, Version 2. 0, 1993.
23. Cundall, P. A., A computer model for simulating progressive large scale movements in blocky rock system. *Proceedings of the Symposium of the International Society for Rock Mechanics*, Nancy, France, 1971, **1**(II-8), 128–132.
24. Lemos, J. V, Hart, R. D. and Cundall, A., A generalized distinct element program for modeling jointed rock mass. In Proceedings of the International Symposium on Fundamentals of Rock Joints, Bjorkliden, 1985, pp. 231–244.
25. Cundall, P. A and Hart, R. D., Numerical modeling of disconuita. *Comprehensive Rock Engineering*, 1992, **2**, 231–244.
26. Souley, M., Hoxha, D. and Homand, F., Distinct element modelling of an underground excavation using a continuum damage model. Submitted to North American Rock Mechanics Symposium, 3–5 June, 1998, Cancun, México.
27. Read, R. S. and Martin, C. D. Technical summary of AECL's mine-by experiment phase 1: Excavation response, AECL-11311, COG-95-171, 1996.
28. Martin, C. D., Read, R. S. and Martino, J. B., Observation of brittle failure around a circular test tunnel. *International Journal of Rock Mechanics and Mining Sciences*, 1997, **34**(7), 1065–1073.
29. Shao, J. F. and Khazraei, R., A continuum damage mechanics approach for time independent and dependent behaviour of brittle rock. *Mechanics Research Communications*, 1996, **23**(3), 257–265.